REPORT

Tsunami hazard analysis in Greenland

TSUNAMI SIMULATIONS IN THE VAIGAT SOUND

DOC.NO. 20210737-02-R
REV.NO. 0 / 2022-09-02

NORWEGIAN GEOTECHNICAL INSTITUTE
NGI.NO

Project

Project title:	Tsunami hazard analysis in Greenland
Document title:	Tsunami simulations in the Vaigat Sound
Document no.:	20210737-02-R
Date:	2022-09-02
Revision no. /rev. date:	0 /

Client

Client:	GEUS - De nationale geologiske undersøgelser for Danmark og Grønland
Client contact person:	Jens Jørgen Møller
Contract reference:	Signed CTR 2022-01-03

for NGI

Project manager:	Finn Løvholt
Prepared by:	Sylfest Glimsdal and Finn Løvholt
Reviewed by:	Sylfest Glimsdal and Carl Harbitz

Executive Summary

Since the mid-20th century, several large volume rock landslides have generated tsunamis in western Greenland. Hence, landslide tsunamis pose a significant hazard to several coastal communities in the region. Examples of past tsunamis include the fatal Karrat fjord 2017 event, as well as several tsunamis in the Vaigat Sound, including two events in Paatuut in 1996 and 2000. A somewhat smaller event in Niiortuut 1952 is also noted. It is important to use the evidence from these past events when preparing methods for future hazard quantification.

Based on a request from GEUS, NGI has performed a set of analysis for landslide tsunamis in the Vaigat Sound. The following work has been carried out:

i) A revision of the modelling scheme used for landslide and rock avalanche tsunamis, updating the methods previously used for modelling the 2017 Karrat fjord event.
ii) Modelling of past tsunamis in Vaigat, including model calibration matching the results to the tsunami observations for the three events Paatuut 2000, Paatuut 1996, and Niiortuut 1952.
iii) Based on the modelling of the past events, ranges for the model input parameters are established, and the selection process for input parameters to be used in hazard analysis is outlined.
iv) A potentially unstable volume identified by GEUS near the abandoned mining village of Qullissat has been analysed with respect to its tsunami hazard potential towards the two villages of Saqqaq and Qeqertaq.

The analyses of the past tsunamis in Vaigat give model results in close agreement with observed run-up heights, primarily focussing on the most solid tsunami observations that are found in Qullissat and Saqqaq. Computer models considering the landslide dynamics as well as tsunami generation, propagation, and inundation, have been used for this purpose. The model results are sensitive to the input parameter values of the landslide dynamics model. Specifically, it is found that the tsunami generation is most sensitive to the resistance properties of the landslide model (friction angle and viscous resistance), and to factors related to changes in the volume and the frontal area impacting water (a volume factor), in addition to the landslide volume itself.

The past events in Vaigat have different tsunami footprints. The most impactful was the 2000 Paatuut tsunami caused by a landslide having a volume > 50 Mm^3. The resulting tsunami produced at least a 12 m high run-up in Qullissat and caused significant inundation in the village of Saqqaq. The similar landslide volume taking place four years earlier in 1996 produced a tsunami with a run-up height not exceeding 4 m. Calibration of the models to match the observations of these events shows that the landslide parameters can vary significantly between two different events. This further reflects how different landslides can have different tsunami-genic potential, and that there is uncertainty associated to the landslide tsunami hazard.

The different landslide parameters that give matching model results for the past events are also suggested as input into selection procedures for the future hazard. A range of parameter values representing the landslide dynamics with at least two end members reflecting this natural variability should be employed. In addition, it is suggested to use run-out statistics of past landslides to guide the parameter value selection process for future hazard analysis. This selection process has previously been used for estimating the tsunami hazard of the potentially unstable slope of Kigarsima in the Uummannaq fjord system, and are in this report also used to estimate the tsunami potential due to the Qullissat scenario.

The landslide dynamics and tsunami due to a 29 Mm^3 potentially unstable soil volume located close to the abandoned town Qullissat has been modelled, for a situation given that the entire volume would fail and develop into a landslide. The volume is located about 2-3 km from the shoreline. Analysis of past landslides with similar volumes suggests that the likelihood of a significant part of the landslide would reach the shoreline is low. In agreement with GEUS, two scenarios were selected for the modelling. In both scenarios relatively low landslide resistance parameter values are used as input, consequently giving relatively long modelled landslide run-out distances. For the first scenario, the landslide does not reach the shoreline. For the second scenario, a fraction of the landslide volume impacts the water body. The modelled inundation range for the second scenario in Saqqaq was 0.5 – 1.5 m without added tide. In Qeqertaq, the tsunami inundation of the second scenario is minor with wave amplitudes less than 0.5 m. Scenario analyses for lower friction values would produce larger tsunamis, but it is believed that the likelihood of events with such a long run-out distance is very low. It is stressed that the probability of release for the various volumes is not assessed in this report. It is also stressed that there may be other slopes that may potentially generate tsunamigenic landslides or rock avalanches, not assessed in this report.

Contents

Table

Figure

Appendix

Review and reference page

1 Introduction

Since the mid-20th century, several major landsides and rock avalanches have generated tsunamis in western Greenland, and some of these have had significant impact and devastating consequences. The most recent major event is the 2017 Karratfjorden rock avalanche and tsunami, which caused four fatalities in the village of Nuugaatsiaq. The Karratfjorden event has been analysed previously by NGI (2021).

In the Vaigat region in western Greenland, several tsunamis have taken place since 1950, including two major landslides in Paatuut in 1996 and 2000, as well as a somewhat smaller event in Niiortuut in 1952. All these landslide induced tsunamis impacted the now abandoned mining town of Qullissat and the surrounding region. The highest tsunami run-up from these events was produced by the 2000 Paatuut tsunami that ran up at least 12 m in Qullissat and also caused significant inundation in the village of Saqqaq. The impact of a tsunami due to a possible rock slope failure is primarily linked to the volume of the landslide and the distance from the source, but also to other factors such as the landslide dynamics and the geometric setting. In particular, the landslide dynamics is a source of uncertainty. It is important to quantify this uncertainty when assessing tsunami hazards.

The by far most commonly established method for analysing the hazard is to simulate the tsunami propagation and inundation by use of numerical methods. By simulating different landslide scenarios, the hazard analysis methods can also be used to quantify the tsunami uncertainty (Løvholt et al., 2020). To calibrate the numerical models, reduce bias, and provide input to future hazard and uncertainty estimation, the past landslide and tsunami events constitute an important basis. In this report, the past events are analysed by simulating all the above-mentioned events in the Vaigat region, taking into account the rich availability of field evidence, both in terms of the observed landslide volumes, geometry, and final run-out distance, as well as traces of tsunami inundation in various locations.

NGI has been contracted by GEUS to analyse the past tsunami events in Vaigat. The hindcasting constitutes a basis to understand implications for modelling the future hazard posed by potential landslides in Greenland. To this end, the methodology for analysing landslide tsunamis has also been expanded compared to the previous analysis (NGI, 2021). Through the hindcasting, rough uncertainty ranges for the parameters describing the landslide dynamics and resulting tsunami inundation heights are discussed. The analysis herein is then further assessed by also drawing upon experience from the analysis of the 2017 Karratfjord tsunami (NGI, 2021). Statistical data such as H/L ratios (a measure of the landslide drop height H to run-out distance L) is also used to guide the analysis.

In addition to hindcasting past events, a potentially unstable rock slope close to Qullissat has been analysed with respect to potential future hazard towards the villages of Saqqaq and Qeqertaq. The probability of the scenario is not assessed in this report.

The present report is organised as follows: Section 2 summarises the historical events in Vaigat to be analysed in this report. Section 3 discusses the model setup, calibration procedures, and sources of uncertainty, noting that the models are further detailed in Appendix A. Section 4 gives results of modelling the past events, while the implications of the modelling for hazard analysis is discussed in Section 5. In Section 6, hazard analysis of a potential landslide event located near the now abandoned town of Qullissat towards Saqqaq and Qeqertaq is described, while a short summary of the findings from this report is finally given in Section 7.

2 Past tsunami and potential events in Vaigat

As noted above, at least two major landslides in Paatuut in 1996 and 2000, as well as a somewhat smaller event in Niiortuut 1952 (Figure 1) have produced tsunamis in Vaigat. In addition, there are other major landslides that did not produce tsunamis, such as the 2021 Assapaat landslide that barely reached the shoreline, but these non-tsunamigenic events have not been analysed here. A summary of the main characteristics of these events are given in Table 1, including the identified initial volume of the landslide, rough estimates of the run-out distances, and tsunami run-up heights in the three locations of Qullissat, Saqqaq, and Qeqertaq. In addition, tsunami observations obtained via remote sensing measurements have been obtained for some uninhabited locations along the fjord shoreline. The observations from these additional locations are associated with higher uncertainty than the observations in Qullissat, Saqqaq, and Qeqertaq.

It is stressed that despite the similar volumes, the Paatuut 1996 and 2000 events produced very different inundation heights. The landslide in 1996 ran down on top of a talus material that was partly eroded and transported down slope by the avalanche. The subsequent 2000 Paatuut landslide then ran down on a base that the 1996 event had already eroded. Paatuut 1996 also had a shorter run-out distance (the exact run-out is not known as the landslide mass is mixed with Paatuut 2000). In addition, a significant fraction of the landslide mass in 1996 did not enter the fjord, as revealed by the presence of large blocks onshore. Part of the scope of this report is to shed light on why these apparently similar volumes produced significantly different tsunami run-up heights.

Table 1: Key information of past tsunami events in Vaigat.

	Volume [Mm^3]	**Landslide run-out distance [m]**	**Maximum run-up height [m] Qullissat**	**Maximum run-up height [m] Saqqaq**	**Maximum run-up height [m] Qeqertaq**
Paatuut 2000	55	7600	12	3	1
Paatuut 1996	57	< 7600	2-4	-	-
Niiortuut 1952	6	800	2	-	-

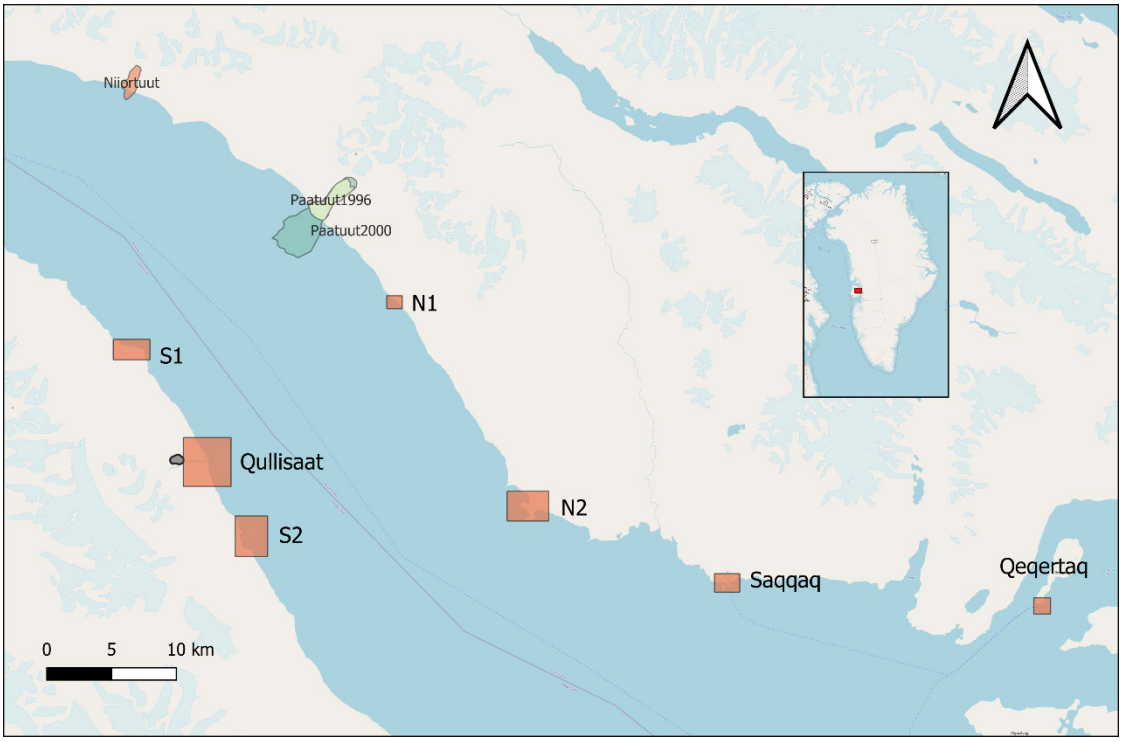

Figure 1: Overview of past landslides and areas for calculation of the tsunami inundation (orange boxes). The potential landslide at Qullissat (initial volume) is marked with grey colour.

3 Model setup

3.1 Main modelling steps

The modelling of the landslide tsunami includes the various steps briefly explained in the bulled list below. The steps are explained in detail in Appendix A.

- Establishing the initial geometry and volume of the landslide.
- Numerical simulation of the landslide dynamics using the initial rock volume as initial condition.
- For each landslide advance below sea, step-wise model the change in sea surface due to the volumetric displacement of the landslide. This serves as a time dependent source model as input to the tsunami propagation model.
- Simulate the tsunami propagation in the fjord.
- For a site of interest such as a populated village, perform dedicated inundation simulations on high resolution topography (5-10 m resolution).

3.2 About model calibration and uncertainty

As outlined in Appendix A, the physics of landslide tsunamis is very complex, and simplifying assumptions in the modelling approach is necessary to make the analysis

feasible. The main uncertainty factors lie in the treatment of the landslide dynamics and the tsunami generation process. To this end, an important part of this report is therefore to use the analysis of the past tsunami events to calibrate the landslide parameter values to match the observations of the past events. These landslide parameter values will obviously still involve a certain degree of uncertainty, which originate partly from natural variability such as slope conditions (aleatory variability) and partly from modelling uncertainty (epistemic variability).

As a basis for this report, a large set of numerical tsunami simulations of the past events in Vaigat has been carried out. For each simulation, the results have been compared with observations of each event. As we are primarily interested in the methods for estimating the tsunami hazard, emphasis has been made on matching observed tsunami run-up from the past events. As discussed in Appendix A, the model simplifications imply that, in order to optimize the model towards the tsunami inundation, some bias in modelling the landslide run-out distance is expected. Most often, this implies that the simulated run-out distance will exceed the field observations, i.e., that the model simulations move further than the field evidences suggest. This is necessary because the tsunami inundation and landslide run-out distances cannot be optimized at the same time with the present model formulation. The reason for this is elaborated further in Section 5.2.

In the present analysis, main emphasis is given on presenting a limited set of analysis where the simulations match the observations. This is used as a basis for the hazard analysis. On the other hand, a more rigorous formal uncertainty analysis is beyond the scope of this report.

3.3 Key terms that may be used in this report

- **Maximum inundation height:** The maximum water elevation onshore above mean sea level during the entire tsunami inundation process.
- **Trim line:** Locations of the innermost inundated (wet) point during the tsunami inundation process.
- **Horizontal inundation length:** Horizontal distance from the shoreline to the trim line (measured along the inundation path).
- **Run-up height:** The vertical tsunami height measured above mean sea level at the trim line location.
- **Maximum water elevation:** The maximum water elevation offshore above mean sea level at a given location.
- **Surface elevation:** The vertical elevation of the water surface offshore measured against the mean sea level.
- **Wave height:** Vertical height of the wave offshore measured from trough to crest.
- **Flow depth:** The water height relative to the topographic level.
- **Wave period:** The duration of a full tsunami wave cycle.
- **Landslide run-out distance:** Horizontal travel distance reached by the landslide.
- **Friction angle (φ):** Here, landslide parameter describing the flow resistance in the numerical model; a low friction angle gives a lower resistance to flow and thus higher landslide velocities and longer runout distance.

- **Viscous drag parameter (ξ):** This is a parameter describing the viscous fluid resistance (air and water) providing resistance to the landslide due to viscous forces in the landslide model.
- **Volume factor (b):** This is a factor describing increase in landslide volume applied in the landslide model. The factor is relative to initial landslide volume on the unstable slope. The factor takes into account the following three effects: The bulking factor of the landslide (inclusion of fluid into the slide body). The entrainment of slope material being picked up by the landslide. The cavity effect of the landslide impacting water.

4 Simulation of past events

A broad set of several parameter combinations was used and combined in the simulations, involving the friction angle φ, the viscous resistance parameter ξ, and the volume factor b, as well as simulations with and without buoyancy. The following parameters were tested (the parameter values found most relevant based on the model vs field observation comparisons are highlighted in **bold**):

- Friction angles: φ=2°, 3°, **5°, 10°,** 15°
- Viscous resistance parameters: ξ=500, 1000, **2000, 5000**, 10000. It is stressed that a high value of ξ implies a low resistance to flow, i.e., higher velocities and longer runout distances.
- Volume factors: b=1.0, **1.25, 1.5**, 1.75
- Simulations **with** and without buoyancy due to the landslide submerged weight

4.1 Paatuut 2000

As discussed above, the year 2000 Paatuut landslide took place after a similar sized event had already occurred in 1996, but the tsunami run-up was significantly higher. The initial landslide volume configuration provided by GEUS is presented in Figure 6, upper left.

Below, we show results for a subset of the analysis for some of the parameter value combinations, focussing on the results that provide the closest agreement with the observational data. To this end, emphasis is given primarily to presenting the simulations matching the observed run-up most closely, but also to the results matching the landslide run-out distance. In addition, we briefly illustrate sensitivity to some of the most important model parameters.

Figure 2 compares the simulated trim lines for the 2000 Paatuut landslide in Qullissat for different combinations of the values of volume factor, friction angle, and viscous resistance parameter with the field observations. Inspecting these comparisons in Figure 2, we arrive at the following findings:

- A landslide model friction angle of 5° is necessary to provide a close match with the observed tsunami trim line. A 10° friction angle gives too low simulated inundation heights.
- A relatively high volume factor (**b**=1.5) and a low viscous resistance (a high value of ξ = 5000) is necessary to provide a close agreement with the observed inundation height. There is some apparent slight underestimation in the northern part of the domain for this combination, but the degree of agreement is still deemed quite good.
- Other parameter combinations give somewhat lower modelled inundation heights than the field observations. Hence, it is necessary to include in the modelling (i) significant extra volume added to the initial landslide (e.g. **b**=1.5) and (ii) a low viscous resistance (e.g. ξ=5000) to match observed data.
- As shown in Figure 2, the results are clearly sensitive to all the variable landslide parameters **b**, φ, and ξ.

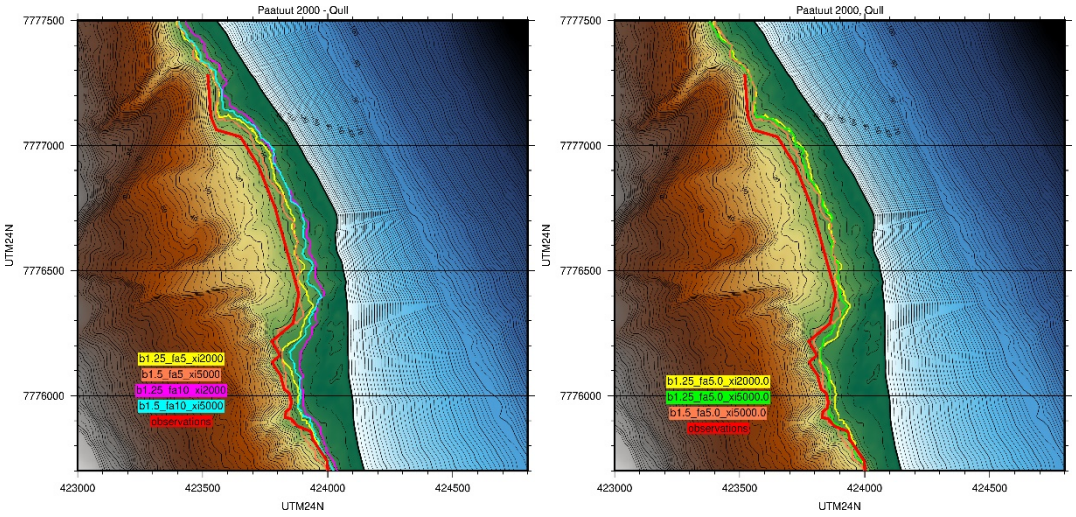

Figure 2: Trim lines for different parameter value combinations modelling the 2000 Paatuut tsunami in Qullissat. Left panel, trim lines for different combinations of volume factors (denoted "b"), friction angles (denoted "fa"), and viscous resistance forces (denoted "xi"). Right panel, similar result representation, showing the sensitivity to the friction angle and volume factor. The trim line derived directly from field observations is shown with red curves.

Figure 3 compares simulated trim lines for the 2000 Paatuut landslide in Saqqaq and Qeqertaq for different parameter combinations of the volume factor, friction angle, and viscous resistance parameter, with the field observations. The comparisons between the simulations and observations here show a different pattern from the respective comparisons in Qullissat:

- In Saqqaq, simulations with higher landslide resistance forces give the best agreement with observations. A combination of the parameter set **b**=1.25, φ=5°, and ξ=2000 gives the better match with observations. Using a friction angle of 10° also gives a good agreement, but as indicated above, using this parameter

value implies a clear underestimation in Qullissat. Oppositely, the parameter combination with best match for Qullissat clearly overestimates the maximum inundation height in Saqqaq.

- In Qeqertaq, there is a tendency to underestimate the observed run-up height, although the parameter combination **b**=1.5 and ξ=5000 gives a reasonably good agreement. On the other hand, the observed run-up here was relatively low, sparsely observed, and hence more uncertain.

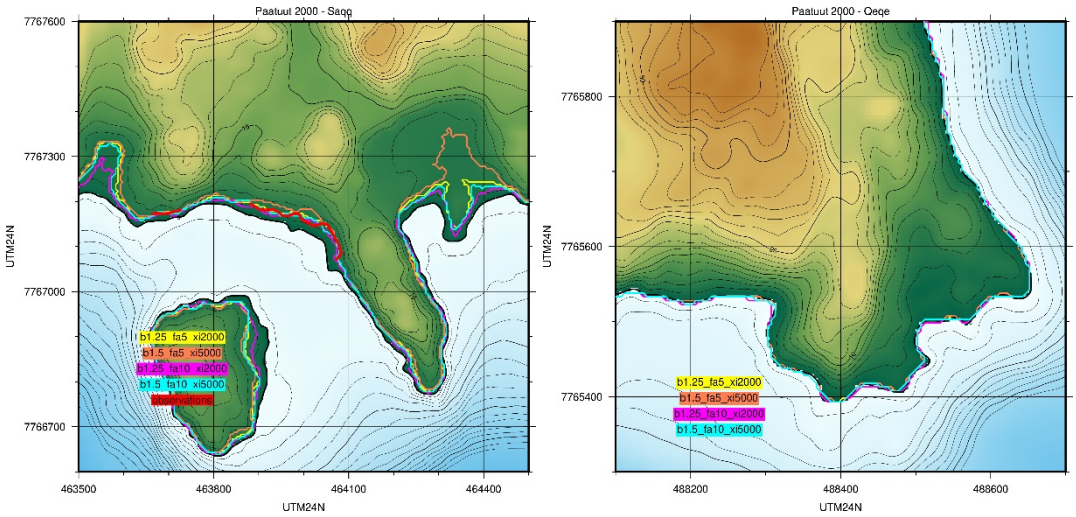

Figure 3: Trim lines for different parameter combinations modelling the 2000 Paatuut event for the inundation areas at Saqqaq (left) and Qeqertaq (right). The figure legends indicate the different combinations of volume factors (denoted "b"), friction angles (denoted "fa"), and viscous resistance forces (denoted "xi") in the simulations.

Figure 4 and Figure 5 compare the simulated trim lines due to the 2000 Paatuut landslide in the uninhabited coastal sites named S1, S2, N1, and N2 (see Figure 1 for locations) for different combinations of the values of volume factor, friction angle, and viscous resistance parameters, together with rough sketches of the trim lines for the field observations. It is stressed that tsunami observations in these sites are based on remote sensing observations and hence much more uncertain than in Qullissat and Saqqaq. Topography data used for the inundation modelling are also less accurate. Hence, the comparisons should be interpreted as much less accurate than those presented above. Nevertheless, the following findings are made:

- The simulations generally tend to underestimate the observations somewhat. Deviations are largest close to the landslide impact (S1, Figure 5), but seems to be more convergent at the two more remote locations (S2 and N2).
- The same parameter set that provided closest match with observations for Qullissat also gives the closest agreement here. The match is good in N2 and partly also N1 and S2.
- S1 is located on the opposite side of the fjord, and the landslide is moving in the direction of S1. S1 also displays the largest deviations between observations and simulations. Therefore, the results in S1 are more sensitive to the details in the

landslide dynamics and the directivity of the landslide motion than the results in the other coastal sites investigated for inundation modelling. The other locations are more affected by wave reflection and refraction.

- Some of the field observations show quite variable inundation locally, and the drawn trim lines of the field observations are also relatively rough. Apart from the S1 location and the locally highest observed run-up heights in N1, N2, and S2, the agreement is relatively good for the simulations with highest inundation.

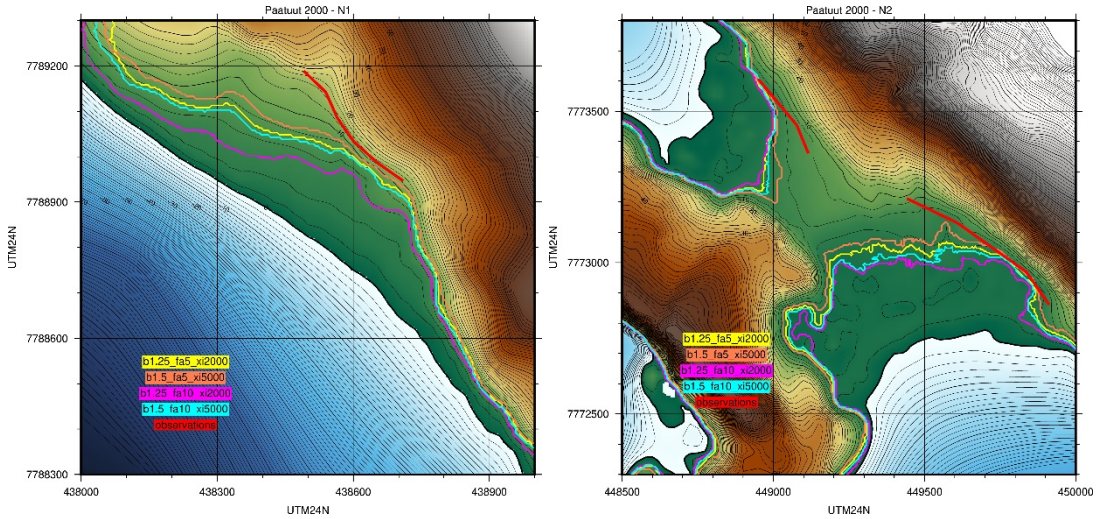

Figure 4: Trim lines for different parameter combinations modelling the 2000 Paatuut event for the inundation areas N1 (left) and N2 (right), see Figure 1 for the positions of N1 and N2. The figure legends indicate the different combinations of volume factors (denoted "b"), friction angles (denoted "fa"), and viscous resistance forces (denoted "xi") in the simulations.

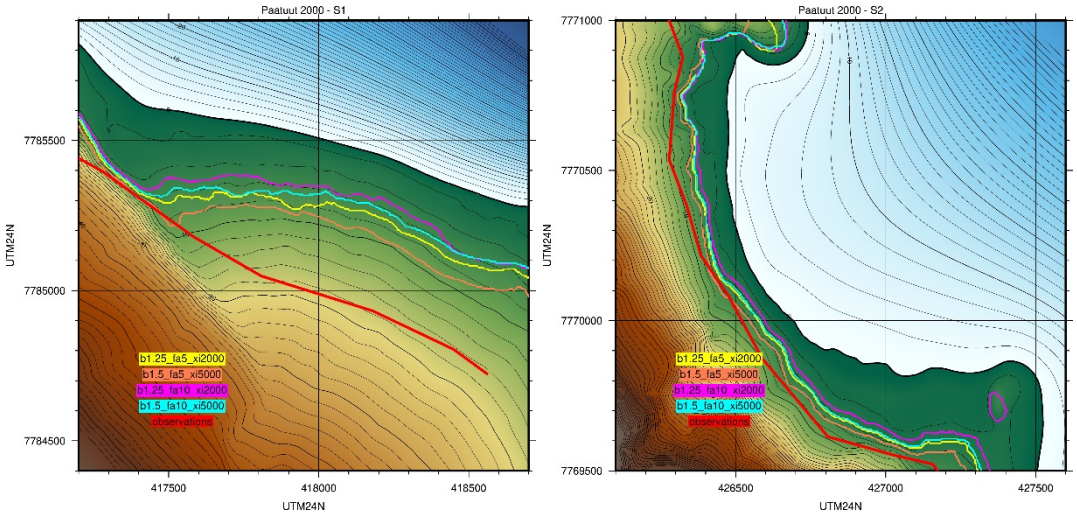

Figure 5: Trim lines for different parameter combinations modelling the 2000 Paatuut event for the inundation areas S1 (left) and S2 (right), see Figure 1 for the positions of S1 and S2. The figure legends indicate the different combinations of volume factors (denoted "b"), friction angles (denoted "fa"), and viscous resistance forces (denoted "xi") in the simulations.

Figure 6 shows the simulated initial landslide configuration and the final run-out distance for three model combinations. Scenarios for volume factors of 1.25 and 1.5, friction angles of 5° and 10°, as well as for ξ values of 2000 and 5000 are shown. All the displayed simulations include buoyancy effects. Figure 6 shows that both the simulations combining lowest volume factor (**b**=1.25) and the highest viscous resistance (low value ξ = 2000), as well as with a high friction angle (φ=10°) with large volume factor and low viscous resistance (high value ξ = 5000) give a close match with the observed final run-out lobe. A low friction angle with either increased volume of the landslide (to **b**=1.5) or decreased the viscous resistance (high value ξ = 5000) implies that the simulated final run-out distance clearly exceeds the observed run-out distance. Another observation from Figure 6 is that apart for the 10° friction angle simulation, all of these landslide simulations move the majority of the landslide masses offshore, and leave very little landslide material behind onshore. As discussed above, there is evidence of large landslide blocks onshore deposited by either the 1996 or the 2000 event. In order to match such observations in the simulations of the Paatuut 2000, it would be necessary use a high friction angle, but this would then imply a pronounced underestimation of the tsunami inundation heights.

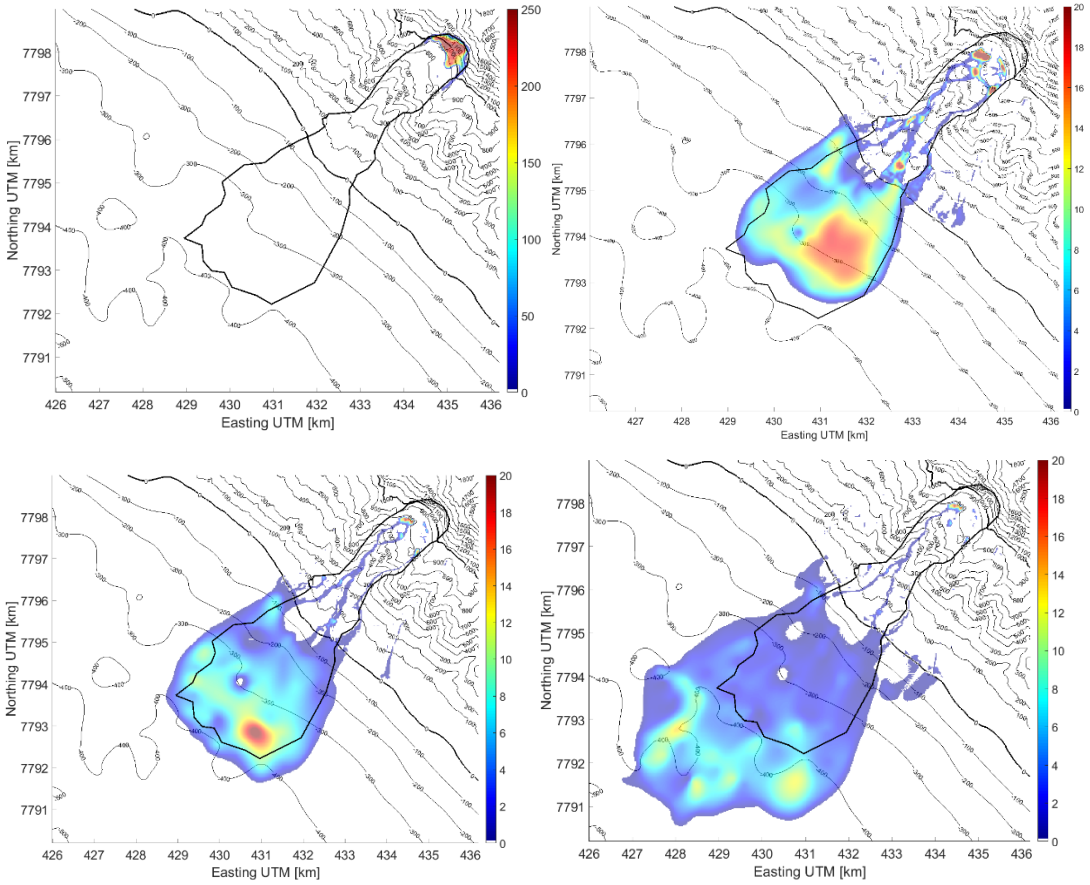

Figure 6: Initial position and observed final runout (provided by GEUS displayed in each figure by the solid black curve) together with simulated final run-out distance for the year 2000 Paatuut landslide. Upper left, initial volume using b=1.25. Upper right, final run-out for b=1.5, φ=10°, ξ=5000. Lower left, final run-out for b=1.25, φ=5°, ξ=2000. Lower right, final run-out for b=1.5, φ=5°, ξ=5000.

4.2 Paatuut 1996

The 1996 Paatuut landslide had similar volume compared to Paatuut 2000, but produced a significantly smaller tsunami. The initial landslide volume configuration provided by GEUS is show in Figure 8.

In Figure 7 the simulated tsunami trim lines for the 1996 Paatuut tsunami are shown for the locations Qullissat and the two uninhabited locations S1 and N1 for different combinations of landslide parameter values. Here, the simulations with the higher friction angle (φ=10°) matches the observed maximum tsunami run-up height in Qullissat best, while landslide simulations with lower friction angles overestimated the tsunami run-up. In S1 and N1, a better agreement with observations is reached using a friction angle of φ=5°. However, as stressed above, the trim lines based on field

observations for S1 and N1 are considered less accurate than those in Qullissat, and we therefore rely more on the comparisons done for the Qullissat location.

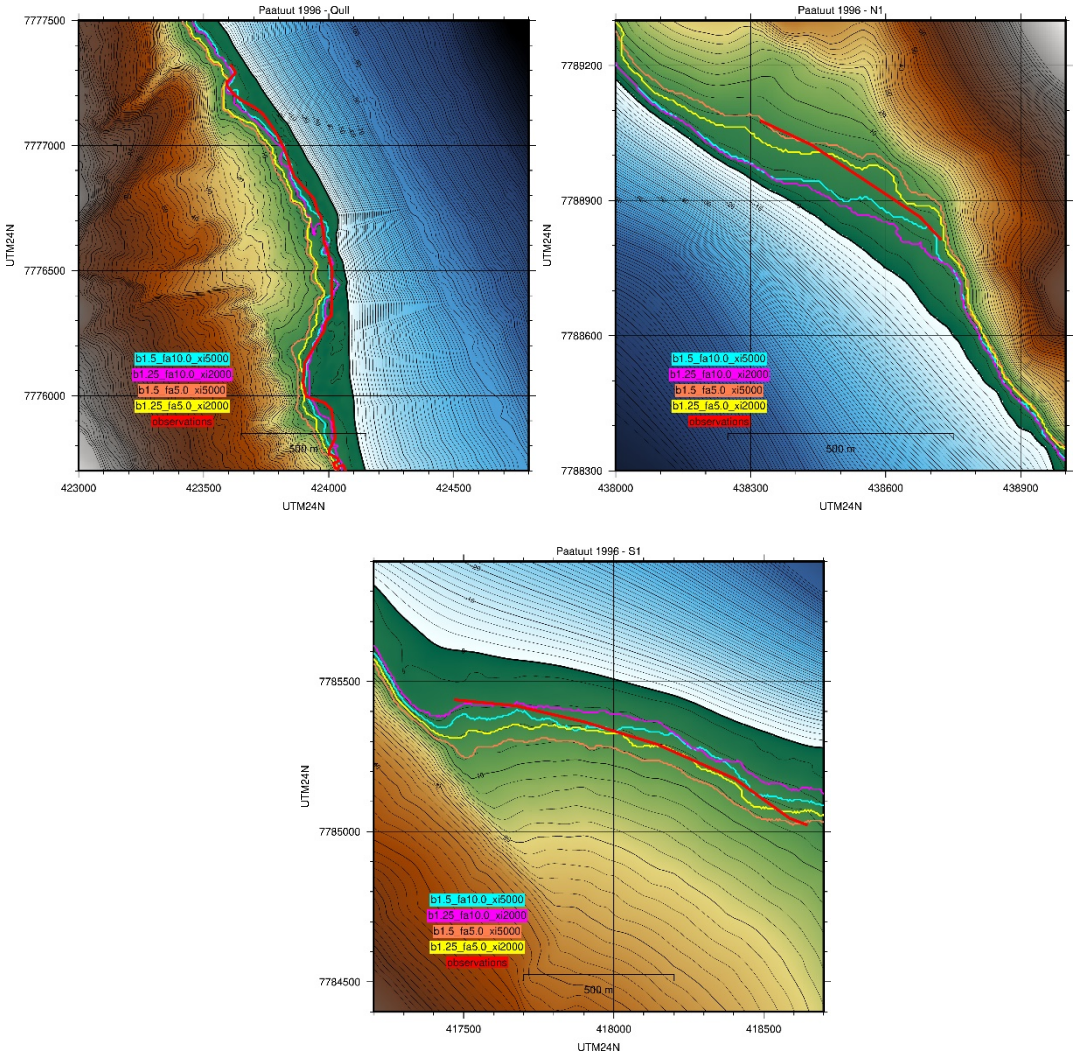

Figure 7: Trim lines for different parameter combinations modelling the 1996 Paatuut event for the inundation areas Qullissat (upper left), N1 (upper right), and S1 (lower). The figure legends indicate the different combinations of volume factors (denoted "b"), friction angles (denoted "fa"), and viscous resistance forces (denoted "xi") in the simulations.

Figure 8 shows the initial landslide location and the simulated final run-out distance for the highest friction angle simulation (φ=10°). This simulation gives a shorter run-out distance compared to the Paatuut 2000 simulations (Figure 6). In this simulation for the 1996 event, there is also more landslide mass left onshore, which agrees with field observations of thick blocky material onshore. In the simulation shown in Figure 8, the thicknesses of the blocks are about 25-30 m thick. There are two reasons for the shorter run-out distance compared to the Paatuut 2000 simulation, the first one is the larger friction angle used for the 1996 model, the second is that the 1996 landslide was initiated further downslope.

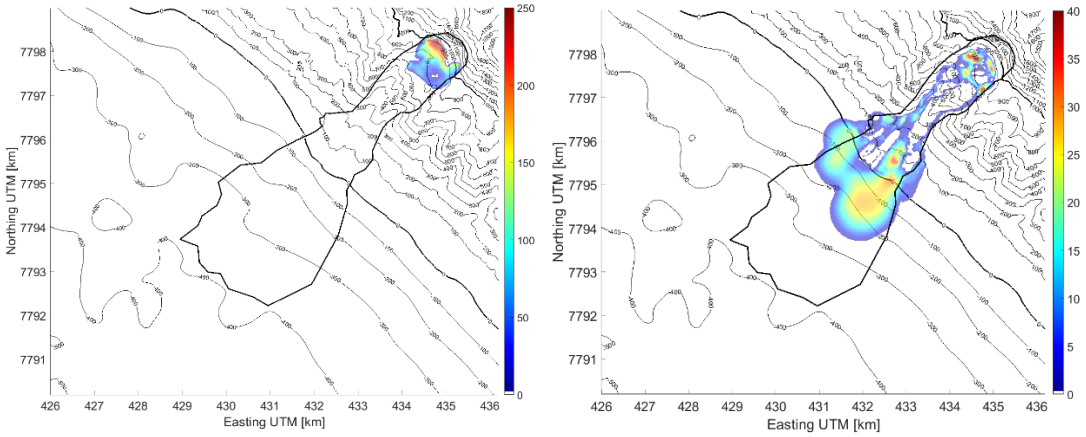

Figure 8: Initial position and observed final runout (provided by GEUS displayed in each figure by the solid black curve) together with simulated final run-out distance for one simulation of the 1996 Paatuut landslide. Left, initial volume. Right, final run-out distance for b=1.25, φ=10°, ξ=5000.

4.3 Niiortuut 1952

Figure 9 shows simulated trim lines for the Niiortuut 1952 using different landslide simulations as input. All simulations without added high tide largely underestimate the observed run-up height (as the event is relatively old, we do not know the tidal level during the event). On the other hand, simulations with added high tide gave good agreement with the observed trim line. The marginally best agreement was obtained with a large volume factor (**b** = 1.5) as well as a low friction angle and viscous resistance (φ=5°, ξ=5000). However, simulations with lower volume factors (**b**=1.25), higher friction angles and viscous resistance (φ = 10°, ξ = 2000) also gave reasonably good agreement. The reason for this is that the additional inundation on top of the tide is relatively modest (as shown by the purple trim line in Figure 9), and the results are therefore not very sensitive to the landslide parameters in the present case. It is important to stress that the observed inundation trim line at Qullissat for the Niiortuut event was similar to the 1996 Paatuut event, and in the comparisons plots it is assumed to be identical to the 1996 event. Yet, it is thus associated with higher uncertainty than the 1996 Paatuut trim line. It is therefore hard to distinguish the model results using different landslide parameters, as the results are not as sensitive to the choice of friction angle as the case was for the two Paatuut events discussed above (both results with φ=5° and 10° gives reasonably good agreement with observations with added high tide).

Figure 10 shows simulated initial landslide volume for the 1952 Niiortuut landslide, as well as the final run-out distance for two different landslide simulations. The simulation with the higher friction angle fits the observed run-out data well, despite having a too wide azimuthal mass distribution, while the simulation with lower friction angles clearly overestimates the run-out distance.

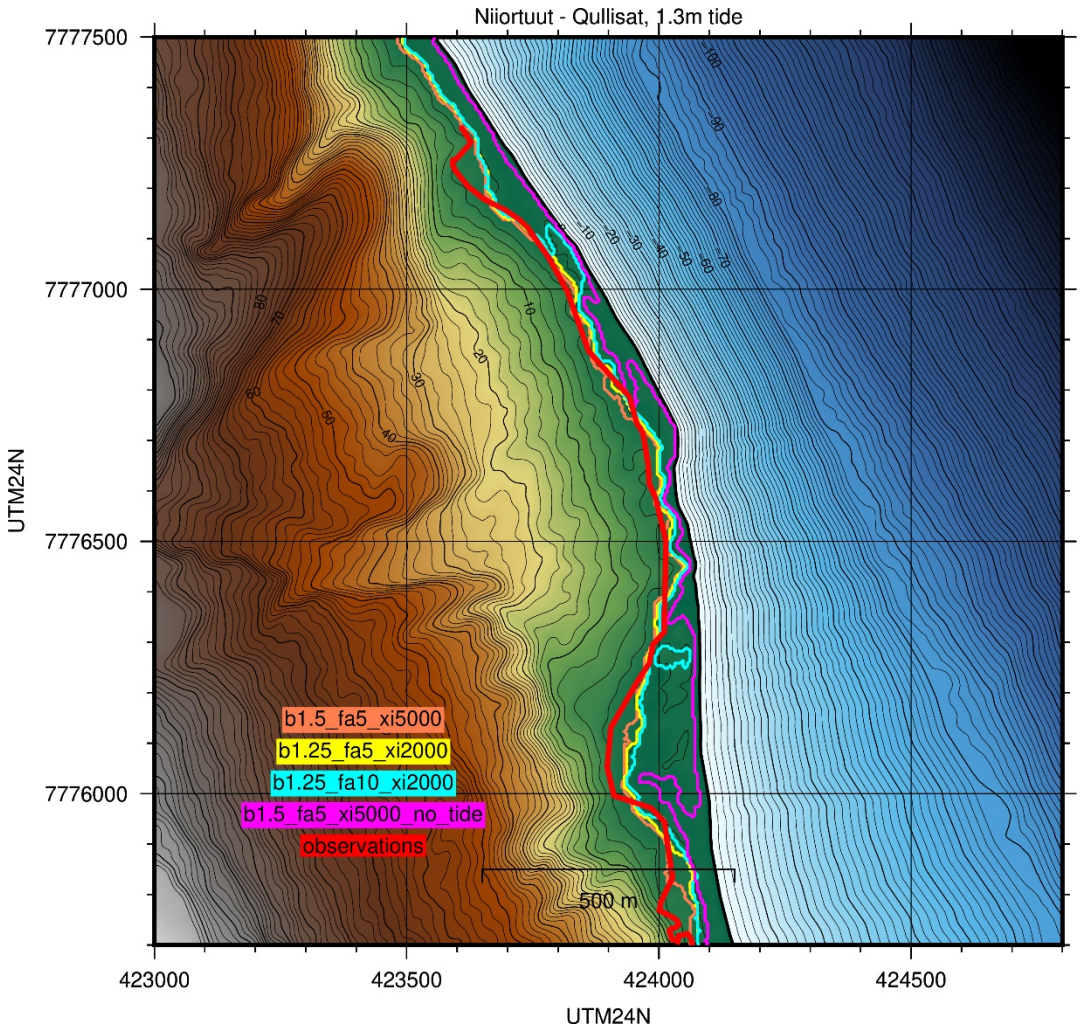

Figure 9: Trim lines for different combinations of parameter values modelling the 1952 Niiortuut event in Qullissat, with a high tide of 1.3 m added. The figure legend indicates the different combinations of volume factors (denoted "b"), friction angles (denoted "fa"), and viscous resistance forces (denoted "xi") in the simulations.

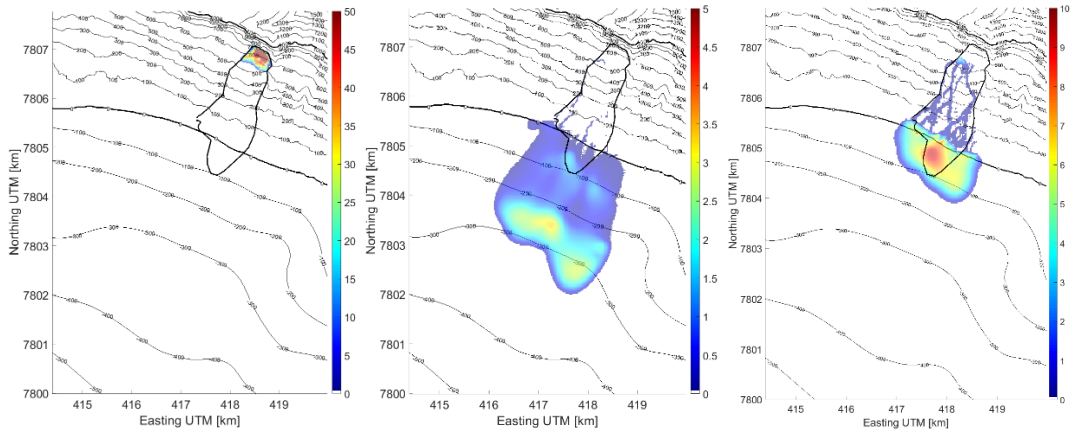

Figure 10: Initial position and observed final runout (provided by GEUS displayed in each figure by the solid black curve) together with simulated final run-out distance for simulations of the 1952 Niiortuut landslide. Left, initial volume, b=1.0. Mid, final run-out for b=1.25, φ=5°, ξ=5000. Right, final run-out for b=1.25, φ=10°, ξ=2000.

5 Discussion

5.1 Comparison with tsunami run-up heights

The modelling of the landslide induced tsunamis in Paatuut 1996, Paatuut 2000, and Niiortuut 1952 presented above, necessitated use of different landslide parameter values in order to match the respective tsunami observations. When assessing the comparison with data, emphasis was made on locations with the most accurate field observations, i.e., especially from Qullissat and Saqqaq. Experience from similar comparisons made for the 2017 Karrat fjord event (NGI, 2021) is also used to establish plausible ranges for the landslide parameter values used for estimating the tsunami hazard. In brief, the following findings are made with respect to selecting landslide parameter values giving the closest fit to the tsunami run-up observations:

- Paatuut 2000: The best fits for Qullissat, Qeqertaq, and the uninhabited fjord locations were obtained with a relatively large added volume factor and low resistance values (**b**=1.5, φ=5°, ξ=5000). For Saqqaq a somewhat higher resistance and a lower volume factor gave a better fit (**b**=1.25, φ=5°, ξ=2000).
- Paatuut 1996: The best fits were obtained using a higher friction angle (φ=10°) than for Paatuut 2000, but otherwise similar landslide parameters (**b**=1.5, ξ=5000).
- Niiortuut 1952: Agreement with (more uncertain) field observation data in Qullissat was only possible by adding high tide to the simulations. Because of the importance of the tide, it is harder to assess the importance of the landslide parameters for this event than for the Paatuut events. Both simulations using friction angles of φ= 5° and 10° gave reasonably close agreement with the observed trim line.

- Karratfjord 2017 (NGI, 2021): The best agreement with observed run-up heights were obtained with a volume factor of b ≈ 1.25 and friction angles φ=5°, 10°, a somewhat lower viscous resistance ξ=10000. It is noted that the tsunami run-up is less sensitive to ξ for high values (e.g. ξ>5000).

It is possible to analyse the comparisons further for the 1996 and 2000 Paatuut landslides:

- The landslide in 1996 ran down on top of a talus material that was partly eroded and transported down slope by the avalanche. The subsequent 2000 Paatuut landslide then ran down on a base that the 1996 event had already eroded.
- It is therefore possible that the already eroded base provided less friction to the 2000 event, which is a possible reason for the better fit using a lower friction angle for Paatuut 2000 (φ=5°).
- In both cases, increased landslide volume after slide initiation was possible: For the 1996 by entrainment of the loose material downslope, and for the 2000 by carrying some of the masses deposited in 1996 further downslope.

5.2 Comparison with landslide run-out distance data

It was necessary to conduct landslide simulations that ran longer than the run-out distances derived from the field observations in order to match the tsunami inundation as discussed in Section 5.1. In turn, landslide simulations matching the observed run-out distance tended to provide too low tsunami run-up height compared to observations. The reason for this is that the friction angle and viscous fluid resistance in the numerical landslide model are represented with constant parameter values representing the motion in both air and water. As the tsunami generation is strongly dominated by the impact of the landslide front entering water, the calibrated fluid resistance will often be dominated by resistance to the motion over land. To match the tsunami generation, the viscous resistance in water will be underestimated, and consequently the simulated run-out distance will often be somewhat overestimated.

Next, we compare run-out of past landslides also from other areas in Greenland. Figure 11 compares simulated and observational H/L ratios. The H/L ratio measures the ratio of the vertical landslide drop height H to the run-out distance L and is a measure of the mobility of the landslide. The H/L ratios typically follow a power law relationship as a function of the landslide volume. As seen from Figure 11, the simulated hindcasts of the different events Paatuut 2000 and 1996 as well as Niiortuut 1952, plot in the lower range of H/L, implying that they generally tend to have longer simulated run-out distances than the observations, which is in agreement with the findings with the individual comparisons between modelled and observed tsunami inundation heights as discussed above. This implies that when selecting the observed tsunami run-up height as the main criterion for matching the simulations, the simulated run-out distance will tend to be in the lower end of the H/L ratio vs volume curve as shown in Figure 11.

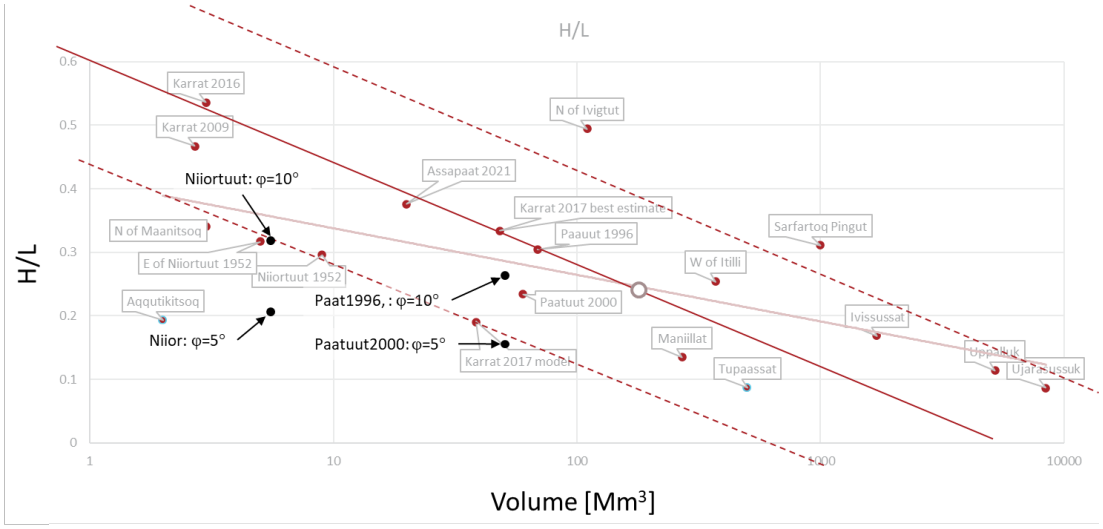

Figure 11: Comparison of the simulated run-out ratios H/L with observational data from past events. The solid red curve and dashed line show the trend and uncertainty in run-out ratio from Norwegian rock avalanche events, while the transparent red curve shows the corresponding trend line fitted to the Greenland events.

The friction angle used for modelling the landslide dynamics is directly related to the H/L ratio, which implies that the friction angle generally decreases when the landslide volume increases (Lucas et al., 2014). It is stressed that Lucas et al.'s relationships are based on run-out of onshore ("dry") landslides, and that subaqueous landslides usually involve a lower friction angle (and longer run-out distances). Based on visual inspection of the curve relating Lucas et al.'s landslide volumes to friction coefficients and friction angles, it is found that a ballpark value of the friction angle in the relevant volume range is ~12-17° (Figure 12) for volumes between 1 and 100 Mm^3 for onshore ("dry") events. These friction angles are slightly higher than some of the 10° friction angle simulations that provided a close match with the final run-out distance for the events analysed in this report. As stressed above, for some events even a 5° friction angle is needed. Such a reduction in friction angle in the fitting process towards tsunami observations partly takes into account reduced friction due to water that is not included in the statistical curve provided by Lucas et al. (2014).

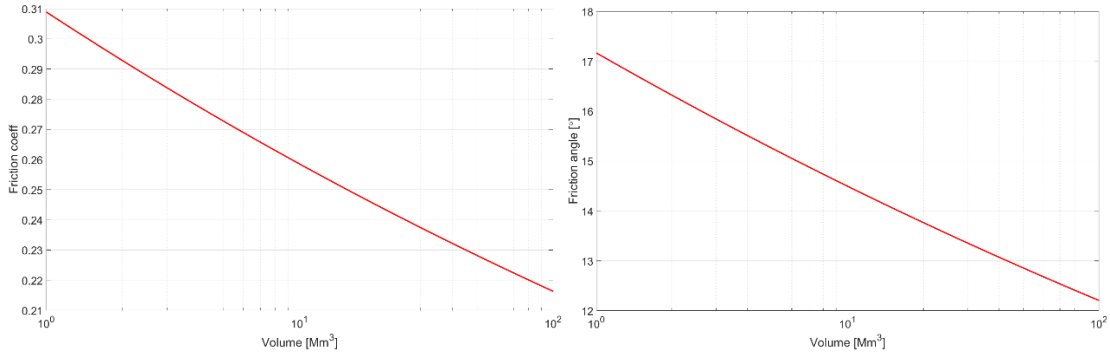

Figure 12: Friction coefficient μ (left) and friction angle φ (right) based on visual inspection of the parametric relationship presented by Lucas et al. (2014)'s Figure 2c. The curves follow the relationship $\mu=A*V^{\beta}$, where a coefficient β=-0.077 was proposed by Lucas et al., A=0.9 was set based on visual inspection of their curve, and V is the landslide volume. The friction angle is given by $\varphi=tan^{-1}(\mu)$.

5.3 Recommended landslide parameter ranges for tsunami hazard analysis in Vaigat

The experience from matching the simulations of the past events above is used to give rough estimates on parameter values for landslide tsunami hazard analysis for the Vaigat region. Ranges for landslide parameter values from high end to low end run-up estimates based on the above comparisons are:

- The friction angle φ used for fitting the model results are in the range 5°-10°, where highest run-up estimates, obtained by fitting the Paatuut 2000 event, are found for the smallest values of φ, and the lowest run-up estimates for the greatest values of φ.
- Volume factors **b** are in the range 1.25-1.5, where highest run-up estimates are found for the greatest values of **b**, and the lowest run-up estimates for the smallest values of **b**.
- Viscous resistance parameters ξ are in the range of 2000-5000, where highest run-up estimates are found for the greatest values of ξ, and the lowest run-up estimates for the smallest values of ξ.

It is stressed that other landslide parameter values may be more relevant for other geological settings than those investigated here. Hence, the values could be subject to change if more information becomes available, for instance from other past landslide tsunami events. It is further stressed that the landslide model parameter values are uncertain, and that usually several sets (at least two) of parameters should be employed for estimating the tsunami inundation uncertainty range.

Where possible, the geological setting should be used to assist the selection of the landslide parameter values. To this end, we note some observations particularly relevant for the landslides in the Vaigat region:

- The presence of talus in many of the areas in Vaigat could indicatively point to similar flow conditions for the landslide as for Paatuut 1996 if a new event were triggered today. This may imply using a high-friction value for new hazard analysis on slopes where no previous rockslides have occurred. On the other hand, we cannot firmly draw the same conclusion based on the analysis of the similar 1952 Niiortuut event, partly because the observations are more uncertain, and partly because the results are less sensitive to the landslide parameters than case was for the two Paatuut events.
- The horizontal distance from the slope failure to the coastline often exceeds several kilometers. Recent landslides such as Assapaat 2021 mainly took place onshore. If a predominant part of the sliding takes place onshore, as was the case with Assapaat, the parameteric relationships derived from onshore deposits (Figure 12) are more directly applicable, and reduction of friction angles based on required tsunami generation and interaction with water can be more limited. When assessing the friction angle to be used in the model, it is necessary to assess this aspect, and provide increased friction angles where the majority or the entire run-out process takes place on land.

6 Hazard analysis for a landslide scenario near Qullissat

An unstable soil volume upslope from the abandoned Qullissat town has recently been detected. The potential release volume is about 29 Mm^3. The material of the mass consists of colluvium, for which friction angles prior to failure typically lie in the range 20-30° (e.g. NVE, 2019). The slope near this volume in Qullissat is about 20°, i.e. below the global friction angles found for this type of soil material. Here, we carry out landslide dynamics simulations for this volume assuming a rock slope failure. It is stressed that the probability of this landslide scenario is not assessed in this report. The location of this rock slope is shown in Figure 13 (left panel).

Based on the calibrations above, two parameter combinations were used to represent the landslide scenarios.

- High friction estimate: Landslide friction angle $\varphi = 10°$ and $\xi = 5000$, with a low **b** = 1.25.
- Low friction estimate: Landslide friction angle $\varphi = 7.5°$ and $\xi = 5000$, with a low **b** = 1.25.

These parameter values were established by a synthesis of combining the hindcasting of the past events in Vaigat presented above, as well as by comparing the simulated run-out ratio H/L with the available statistical data (Figure 14). For the high friction estimate, it was found that the landslide did not reach the water surface, and hence could not generate a tsunami (Figure 13, mid panel). As shown in Figure 14, the run-out ratio for this simulation is in the lower range of H/L compared to the past Greenland events. Hence, the modelled run-out distance for the 10° friction angle is considered to be long

compared to the past mapped past events. We also note that a friction angle of 10° is smaller than the statistically based estimates of Lucas et al. (2014) which is based on onshore events. In addition, most of the mapped past events are partly subaqueous, which implies that the past events are expected to have a higher mobility statistically than this simulated (onshore) Qullissat scenario. Therefore, the likelihood of this landslide scenario reaching the coastline and producing a tsunami is considered low.

To illustrate the effects of uncertainty and investigate the possible tsunami-genesis of this landslide scenario, the results with a slightly lower friction angle (φ=7.5°) were also investigated. The run-out ratio for this event is also on the low end of the statistical distribution. As shown in Figure 13, only a fraction of the landslide volume ran out further than the shoreline. Consequently, the tsunami generation was relatively modest. The maximum simulated tsunami run-up height in Saqqaq were in the range of 0.5 – 1.5 m (see Figure 15), while for Qeqertaq the maximum water level did not exceed 0.5 m, and did hence not represent any significant tsunami. It is noted that scenarios with lower friction (e.g., 5°) will produce higher run-up, but due to their excessively low H/L ratios such events were considered increasingly more unlikely.

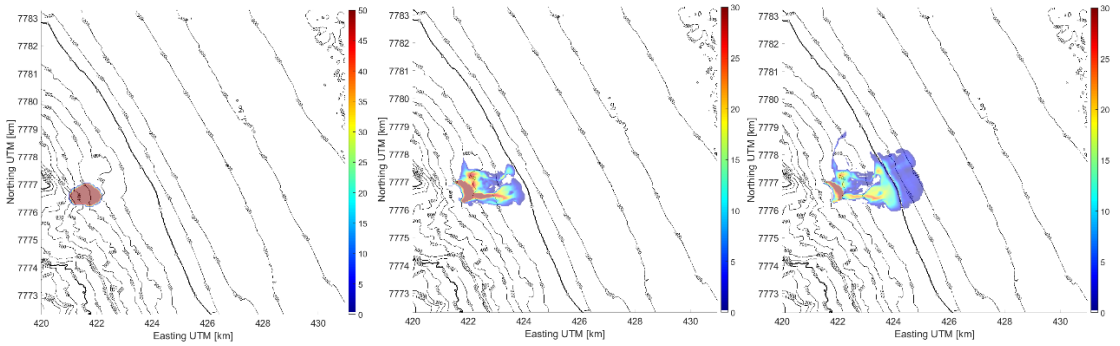

Figure 13: Initial position (provided by GEUS) and simulated final run-out distance for simulations of the potential Qullissat landslide. Left, initial volume, b=1.25. Mid, final run-out for b=1.25, φ=10°, ξ=5000. Right, final run-out for b=1.25, φ=7.5°, ξ=5000.

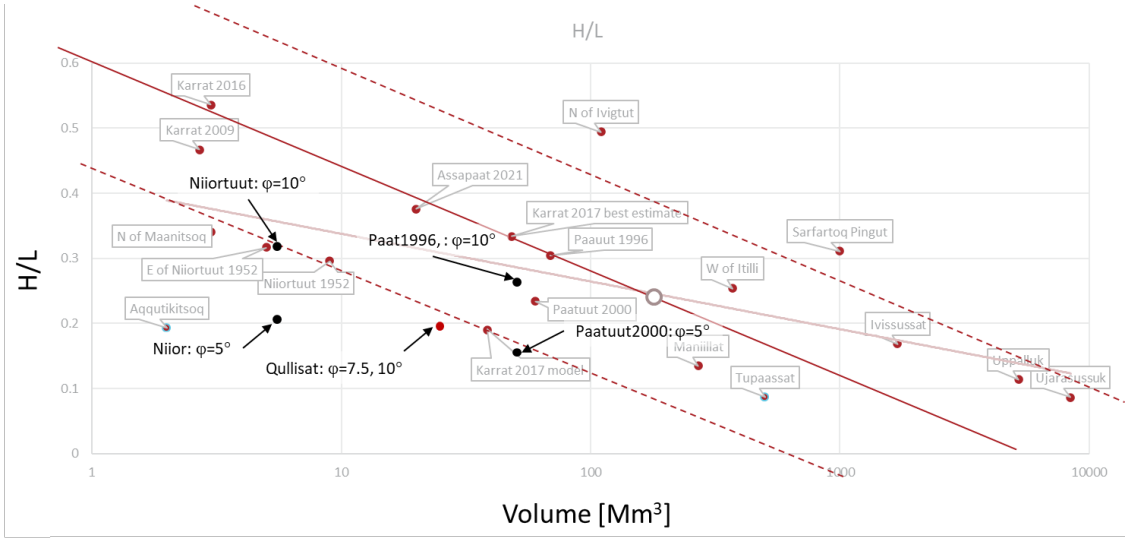

Figure 14: Comparison of the simulated run-out ratios H/L for the two simulated Qullissat scenarios presented in this report with past events.

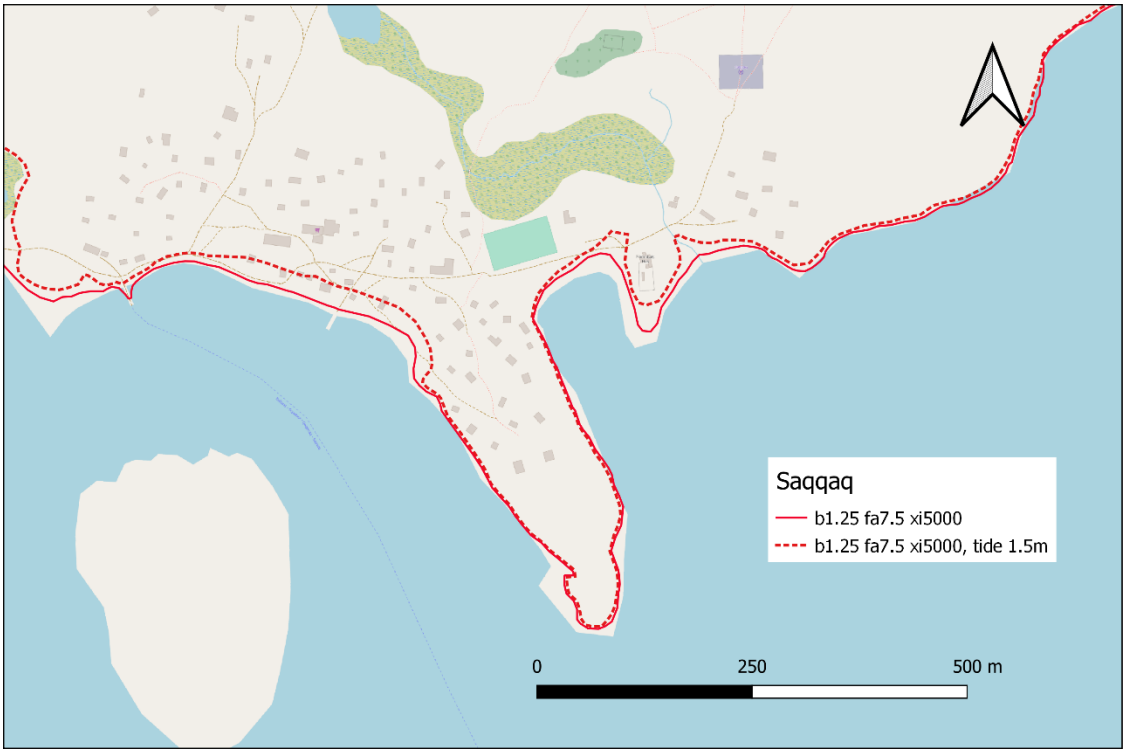

Figure 15: Trimline for Saqqaq with and without added high tide for the 7.5° induced friction angle simulation Qullissat scenario.

7 Concluding remarks

In this report, a set of previous landslide tsunamis have been simulated in order to calibrate the model parameter values and thus provide rough guidelines for future hazard analysis for landslides in western Greenland and Vaigat in particular. In concrete terms, it forms the background for selecting parameters for assessing the potential Kigarisma rock avalanche tsunami hazard (NGI, 2022) as well as the present hazard analysis for a potential unstable slope close to Qullissat.

The following past landslide events have been investigated in this report:

- Paatuut landslide and tsunami 2000
- Paatuut landslide and tsunami 1996
- Niiortuut landslide and tsunami 1952

The procedures for simulating landslide tsunamis involve simulating landslide dynamics as well as tsunami generation, propagation, and run-up (as described in Appendix A). Moreover, the procedures for simulating the landslide dynamics have been updated to take into account buoyancy and volume increase of the landslide during flow. The main factors controlling the tsunami generation are the parameters describing the landslide dynamics. The subset of the landslide parameters most strongly affecting the tsunami generation was identified to be:

- The friction angle in the landslide model. The calibration herein suggests a range 5-10°, where the 5° angle is obtained by fitting it towards the Paatuut 2000 event.
- The volume factor, taking into account landslide entrainment, bulking factors (mixing of the landslide with surrounding fluid), and tsunami generation effects (cratering). The calibration herein suggests a range 1.25-1.5.
- The viscous resistance to the flow exerted by the surrounding fluid on the landslide. The calibration herein suggests a range 2000-5000 m/s^2.

These established parameter ranges are based on events in western Greenland and in the Vaigat region in particular, but still seem to roughly correspond also closely with statistical analysis of past landslides from other regions. The parameter selection puts emphasis on the tsunami generation. All the landslides considered here originate onshore, but all of them would not necessarily reach the shoreline. Therefore, the parameter selection should carefully examine the potential for whether or not a significant part of the landslide will be subaqueous.

The tsunami hazard due to a potential 29 Mm^3 landslide located close to the abandoned town Qullissat has been examined through numerical modelling. By comparing the landslide volume and slope with statistics of past landslides, it is found that the likelihood of the landslide impacting water is small, but that there is a potential for generating a tsunami even if should the landslide happen. Two scenario simulations were conducted. The first scenario (friction angle 10°) does not reach the shoreline, while for the second scenario (friction angle 7.5°) a fraction of the landslide volume reaches the

fjord, thus generating a tsunami. The simulated run-up height of this tsunami (friction angle 7.5°) in the Saqqaq is 0.5 – 1.5m, while the run-up height in Qeqertaq is less than 0.5 m. It is noted that scenarios with lower friction angle (e.g., 5°) will produce higher run-up than the second scenario, but due to their excessively low H/L ratios such events were considered unlikely. It is stressed that the probability of release for this volume is not assessed in this report. It is also stressed that there may be other slopes potentially holding tsunamigenic landslide or landslides, not assessed in this report.

8 References

Lucas, A., Magneney, A, and Ampuero, J.P. (2014), Frictional velocity-weakening in landslides on Earth and on other planetary bodies. Nat. Commun. 5:3417 doi: 10.1038/ncomms4417

Løvholt, F., Glimsdal, S., and Harbitz, C. B. (2020). On the landslide tsunami uncertainty and hazard. Landslides, 17(10), 2301-2315.

NGI (2021), Tsunami hazard screening for the Uummannaq fjord system – Greenland - Hazard scenario simulations and 2017 event hindcast, NGI report no 20200823-01-R

NGI (2022), Tsunami hazard analysis in Greenland - Runup modelling of potential tsunamis from Kigarsima, 20210737-01-R

NVE (2019), https://publikasjoner.nve.no/veileder/2019/veileder2019_01.pdf

Appendix A

LANDSLIDE AND TSUNAMI MODEL

Contents

A1 Introduction and modelling set up

The main aim of this document is to give a detailed background of the modelling procedure for simulating landslide tsunamis for different scenarios, from landslide dynamics, tsunami generation, to tsunami propagation and finally inundation simulations. This Appendix gives a similar model description as given in the past hazard report for Uummannaq fjord system (NGI report 20200823-01-R) but includes some new methodological features. The most important new additions from the past NGI are that the present modelling includes i) a treatment of landslide buoyancy effects for simulating the landslide dynamics, and ii) an added volume factor that partly takes into account entrainment of landslide mass during landslide progression, mixing of landslide mass with ambient fluids, as well non-linear effects due to cratering during tsunami generation.

The landslide scenarios can have different volumes and material properties, that in turn govern their speed. The tsunamigenic strength of subaerial landslides impacting water typically increases with the landslide volume and speed of the landslide, as well as details related to how the landslide moves. Hence, the tsunami modelling must take into account the rate and extent the landslide motion displaces water. The modelling procedures used in this report follows the descriptions of Løvholt et al. (2010, 2015, 2020), and includes a model for the landslide dynamics (Section A3), a model for conveying the landslide displacement into wave generation (Section A4), a model for the tsunami propagation in the fjord system and open sea (Section A5), and a local tsunami inundation model that takes into account the detailed topography and flow pattern at the study sites (Section A6). The individual models are described in the subsections below. These subsections also describe the modelling set-up, background data, computational grids, etc. In addition, we describe the background datasets for this report in Section A2.

A2 Background, available datasets, and inputs

The following datasets were provided by GEUS and used in the analysis:

- A combined 100 m resolution topo-bathymetry covering the Vaigat strait. This was used to set up the grid for both the landslide dynamics simulations the tsunami propagation model.
- High resolution (0.5 m) topographic data for three of the study sites, namely Qullisat, Saqqaq, and Qeqertaq, which was used to set up the high-resolution topography grids (of 5-10 m resolution) for the local inundation models.
- Initial volume configurations and runout distance (lobe) for the past landslides Paatuut 1996 and 2000, and Niiortuut 1952.
- Observed tsunami inundation trim lines due to the Paatuut 1996 and 2000, and Niiortuut 1952 landslides. The majority of the data are from the Paatuut 2000 landslide.

A3 Landslide dynamics model

The landslide model VoellmyClaw (Kim, 2014) is used to model the landslide dynamics. VoellmyClaw is vertically depth averaged, meaning that the landslide thickness is describe numerically with single cell values for each horizontal coordinate. This model is developed for so called granular type landslides that encompass different types of rheologies including subaerial rockslides.

The Voellmy model is described by two parameters, the friction angle φ, and the quadratic friction coefficient ξ. The quadratic coefficient ξ is used to take into account the viscous fluid resistance acting on the landslide.

The VoellmyClaw model does not take into account buoyancy effects directly, and to model this effect, the slope of the bathymetry is modified to reduce the effective gravity. The slope used for the submarine part of the landslide dynamics is therefore reduced to give a reduced gravity of $0.43 \times g$, where g is the gravitational acceleration, was used here. This corresponds roughly to a landslide density of 1750 kg/m^3.

Effects of entrainment, i.e. mass interaction with the substrata, and mixing of the landslide mass with air and water and, is not directly included in VoellmyClaw. Neither is the effect of the highly non-linear tsunami generation process that includes cratering and strong wave breaking very close to the impact. All of the above effects may increase the effective frontal area of the landslide during water impact, which can increase the tsunami generation. To take these effects into account in an ad-hoc fashion, an added volume factor **b** that incorporates the abovementioned effects by simply increasing the initial landslide volume (by increasing the landslide thickness). It is stressed that this representation assumes that all the mass effects are included contemporaneously when the landslide is release, which represents a simplification.

The landslide dynamics model uses the initial landslide thickness covering the unstable slope area as input. The landslide simulations are carried out on the combined 20 m topo-bathymetric grid provided for the Vaigat region by GEUS. For the landslide simulations, this grid was cleaned up (by interpolating adjacent data into gaps) and cut to encompass the local region around the slide and refined to a 10 m grid resolution. The landslide simulations were carried out up to 300 s, and the landslide thickness was exported every 5 s as the input source for generating the tsunami.

A4 Tsunami generation model

When the landslide moves along the sea bottom, it sets up a water displacement that causes the wave. The tsunami generation model used here takes this effect into account, following the description of Løvholt et al. (2015). This model takes into account the hydrodynamic wave surface response due to volumetric seafloor deformations using full potential theory based on Kajiura's model (Kajiura, 1963), but is different from Kajiura as it is time dependent. Typically, the size of landslide disturbance on the bottom is

distributed over at least 2-3 water depths, which means that the water column acts as a smoothing filter. This process goes on continuously while the landslide is progressing, at each time step of the simulation, continuously updating the surface elevation in the tsunami propagation model (described in Section A5). It is stressed that this model is linearized, and hence does not take into account the splashing and cratering process during the slide impact.

A5 Tsunami propagation model

The linear dispersive tsunami propagation model GloBouss (Pedersen and Løvholt, 2008) is used for simulating the wave propagation in the open sea. GloBouss is depth averaged, and takes into account wave frequency dispersion, which implies that shorter waves travel more slowly than the longer leading wave. Dispersion is particularly important for tsunamis with short wavelengths relative to the water depth, such as those typically induced by subaerial landslides. The short wave-periods reported for the 2017 Karrat fjord tsunami and the late arrival of the maximum waves are both likely partly due to frequency dispersion, and the same is likely to be the case for other landslide tsunamis in western Greenland. The wave generation model described in Section A4 is used as a time dependent source model in GloBouss. In turn model outputs from the tsunami propagation model is used as time dependent input models for the tsunami inundation model as described in Section A6.

A6 Tsunami inundation model

The tsunami inundation model ComMIT (Titov et al., 2011) is employed here for simulating tsunami inundation. The ComMIT program uses the depth averaged non-linear shallow water model MOST (Titov and Gonzalez, 1997) as the computational engine for modelling the local tsunami inundation. MOST simulates the tsunami inundation using high resolution grids in two dimensions. For computational feasibility, a set of so-called telescopic grids with increasingly higher grid resolution and smaller domains are used. The grid with the largest extent has coarser resolution than the next inner grid and so on. In the applications employed here, three levels of grids are applied, and grid levels from coarsest to finest are denoted A, B, and C. The inundation is calculated on the C-grid only, and the hazard analysis is therefore based on the model outputs within this grid. The horizontal resolution of the C-grids used here is 5 m. The ComMIT application includes a dynamic one-way coupling between the offshore tsunami propagation model GloBouss and in the inundation model (Løvholt et al., 2010). In this way, the results from the offshore wave propagation is seamlessly connected to the inundation simulations. The offshore wave propagation then acts as a time dependent forcing of the MOST simulation as a function of time along the periphery of the A-grid. Extents of the C grids used in this report are shown in the outline of the study are in the main body of this report.

A7 Key simplifications in the modelling procedure

As the physics of landslide tsunamis is very complex, including several features that are complicated and resource intensive to model, it is necessary to make some simplifying assumptions in the modelling to make the analysis feasible. The main uncertainty factors lie in the treatment of the landslide dynamics and the tsunami generation process. For a more realistic treatment of all these effects a multi-phase Computational Fluid Dynamics model would be necessary, but such models are too resource intensive to be used in practical hazard analysis. Moreover, they cannot be applied for modelling tsunami wave propagation far from the generation area. Hence, the only practical option is to turn to depth-averaged landslide and tsunami model. In particular the following simplifying factors are deemed important:

- Correction of effective landslide volume with a typical factor for e.g. b=1.25 or b=1.5 to account for:
  - Tsunami generation: A rock avalanche creates a so-called crater formation where parts of the water is thrown up, and this can include strong breaking and turbulence during impact. As the tsunami generation (Section A4) and propagation models (Section A5) are linearised, they cannot take into account the crater generation and the strong non-linearities in the impact. This is partly mitigated by adding the heuristic volume factor **b** that increases the effective landslide volume and frontal area interfacing the water during impact.
  - Bulking factor: The initial volume of the rock avalanche consists mainly of rock or soil material, which will mix with air and water. This mixing process will increase the effective flow volume of the landslide. The additional volume mixed into the landslide volume is referred to as the bulking factor. As variable mass and volume is not accounted for in the applied landslide model, the bulking factor is added through the volume factor **b** that increases the effective landslide volume.
  - Entrainment: The rock avalanche may further erode the substrata and further increase its volume by mobilizing the mass downslope of the initial landslide. This process is referred to as entrainment. Entrainment is not included in applied landslide model, and the entrainment is partly mitigated through the volume factor **b** that increases the effective landslide volume.
- Viscous resistance to flow: The landslide moved through both air and water. The resistance to motion is much higher in water than in air. On the other hand, the landslide model only allows one viscous resistance factor ξ for both air and water. The viscous resistance factor ξ therefore represents an aggregate factor, which is calibrated mainly towards the observed tsunami run-up height. As a major part of the tsunami generation takes place in the early stages just after the landslide has impacted water, it is expected that the parameterised viscous resistance in air controls the wave generation. Hence, the calibrated value of the viscous resistance factor ξ towards tsunami inundation observations may imply that the resistance force while the landslide moves under water is underestimated. Consequently, the landslide may have a too long run-out distance. A result of the model simplification is that when the results are optimized towards the tsunami run-up observations, it is

likely that the model will exaggerate the modelled run-out distance of the landslide as a result.
- Constant landslide properties: All the input parameters of the landslide motion are constant in time and space. Hence, effects that are variable with time, such as internal friction angle due to mixing with water, are not captured.

A8 References

Kajiura, K. (1963). The leading wave of a tsunami. Bulletin of the Earthquake Research Institute, University of Tokyo, 41(3), 535-571.

Kim, J. (2014). Finite volume methods for Tsunamis generated by submarine landslides (Doctoral dissertation, Univ. Washington).

Løvholt, F., Pedersen, G., and Glimsdal, S. (2010). Coupling of Dispersive Tsunami Propagation and Shallow Water Coastal Response. The Open Oceanography Journal, 4(1).

Løvholt, F., Pedersen, G., Harbitz, C.B., Glimsdal, S., and Kim, J. (2015). On the characteristics of landslide tsunamis. Philosophical Transactions of the Royal Society A: Mathematical, Physical and Engineering Sciences, 373(2053), 20140376.

Løvholt, F., Glimsdal, S., and Harbitz, C.B. (2020). On the landslide tsunami uncertainty and hazard. Landslides, 17, 2301-2315.

NGI (2021) – Tsunami hazard screening for the Uummannaq fjord system – Greenland – Hazard scenario simulations and 2017 event hindcast. NGI report 20200083-01-R

Pedersen, G., and Løvholt, F. (2008). Documentation of a global Boussinesq solver. Preprint series. Mechanics and Applied Mathematics http://urn. nb. no/URN: NBN: no-23418.

Titov, V.V., Moore, C.W., Greenslade, D.J.M., Pattiaratchi, C., Badal, R., Synolakis, C. E., and Kânoğlu, U.T.K.U. (2011). A new tool for inundation modeling: Community Modeling Interface for Tsunamis (ComMIT). Pure and Applied Geophysics, 168(11), 2121-2131.

Titov, V.V., and Gonzalez, F.I. (1997). Implementation and testing of the method of splitting tsunami (MOST) model. NOAA technical report.

Kontroll- og referanseside/ Review and reference page

Dokumentinformasjon/*Document information*		
Dokumenttittel/*Document title* Tsunami simulations in the Vaigat Sound		**Dokumentnr./*Document no.*** 20210737-02-R
Dokumenttype/*Type of document* Rapport / Report	**Oppdragsgiver/*Client*** GEUS - De nationale geologiske undersøgelser for Danmark og	**Dato/*Date*** 2022-09-02
Rettigheter til dokumentet iht kontrakt/ *Proprietary rights to the document according to contract* Oppdragsgiver / Client		**Rev.nr.&dato/*Rev.no.&date*** 0 /
Distribusjon/*Distribution* INGEN: Distribueres kun til oppdragsgiver (utvidet konfidensialitet, X prosjekter) / NO: Distribution to client only (extended confidentiality, X projects)		
Emneord/*Keywords* tsunami, modelling, landslide, inundation, run-up, hindcasts		

Stedfesting/*Geographical information*	
Land, fylke/*Country* Greenland	**Havområde/*Offshore area***
Kommune/*Municipality*	**Feltnavn/*Field name***
Sted/*Location* Vaigat Sound	**Sted/*Location***
Kartblad/*Map*	**Felt, blokknr./*Field, Block No.***
UTM-koordinater/*UTM-coordinates* **Zone: East: North:**	**Koordinater/*Coordinates*** **Projection, datum: East: North:**

Dokumentkontroll/*Document control*
Kvalitetssikring i henhold til/*Quality assurance according to NS-EN ISO9001*

Rev/ *Rev.*	**Revisjonsgrunnlag/*Reason for revision***	**Egenkontroll av/ *Self review by:***	**Sidemanns-kontroll av/ *Colleague review by:***	**Uavhengig kontroll av/ *Independent review by*:**	**Tverrfaglig kontroll av/ *Interdisciplinary review by:***
0	Original document	2022-08-26 Sylfest Glimsdal	2022-08-28 Carl B. Harbitz		

Dokument godkjent for utsendelse/ *Document approved for release*	**Dato/*Date***	**Prosjektleder/*Project Manager***
	2 September 2022	Finn Løvholt

NGI (Norwegian Geotechnical Institute) is a leading international centre for research and consulting within the geosciences. NGI develops optimum solutions for society and offers expertise on the behaviour of soil, rock and snow and their interaction with the natural and built environment.

NGI works within the following sectors: Geotechnics and Environment – Offshore energy – Natural Hazards – GeoData and Technology

NGI is a private foundation with office and laboratories in Oslo, a branch office in Trondheim and daughter companies in Houston, Texas, USA and in Perth, Western Australia

www.ngi.no

NGI (Norges Geotekniske Institutt) er et internasjonalt ledende senter for forskning og rådgivning innen ingeniørrelaterte geofag. Vi tilbyr ekspertise om jord, berg og snø og deres påvirkning på miljøet, konstruksjoner og anlegg, og hvordan jord og berg kan benyttes som byggegrunn og byggemateriale.

Vi arbeider i følgende markeder: GeoMiljø – Offshore energi – Naturfare – GeoData og teknologi.

NGI er en privat næringsdrivende stiftelse med kontor og laboratorier i Oslo, avdelingskontor i Trondheim og datterselskaper i Houston, Texas, USA og i Perth, Western Australia.

www.ngi.no

OSLO
TRONDHEIM
HOUSTON
PERTH

NORWEGIAN GEOTECHNICAL INSTITUTE
NGI.NO

Main office
PO Box 3930 Ullevaal St.
NO-0806 Oslo
Norway

Trondheim office
PO Box 5687 Torgarden
NO-7485 Trondheim
Norway

T (+47)22 02 30 00
NGI@ngi.no

BIC NO. DNBANOKK
IBAN NO26 5096 0501 281
ORGANISATION NO.
958 254 318MVA

ISO 9001/14001
CERTIFIED BY BSI
FS 32989/EMS 612006